Zircon and titanite age determinations from igneous rocks in the Karibib District, Namibia: implications for Navachab vein-style gold mineralization

R.E. Jacob[1], J.M. Moore[1], R.A. Armstrong[2]
[1]*Rhodes University, Grahamstown, South Africa*
[2]*Australian National University, Canberra, Australia*

SHRIMP U-Pb dating of single zircon grains from Damaran granitic rocks yielded ages of 550Ma and 540Ma for the Mon Repos diorite and Rotekuppe granite plutons respectively. Single titanite grains yielded a 500Ma metamorphic age for metalamprophyre and an identical age for quartz/skarn veins from the Navachab open pit. Aplite/pegmatite dykes that cut the mineralization give poor apparent ages between 540Ma and 565Ma with large errors. The timing of mineralization remains equivocal, either intrusive-related (550Ma), accepting the pegmatite model age, and subsequently reset by metamorphism, or directly metamorphic (500Ma).

Introduction

Henno Martin was a remarkable man and a most talented geologist with wide-ranging interests in earth science. He recognised that an understanding of mineral deposits is of great importance in the broader context of geological evolution. Fifteen per cent of his seminal book on the Precambrian of Namibia and Namaqualand (Martin, 1965) is devoted to mineral deposits. Much of Namibia's mineralization is located in the Damara Orogen, most of it related to magmatism and/or metamorphism. The Central Zone (Miller, 1983) contains significant magmatic and hydrothermal mineralization, including Li, Be, Sn in pegmatites, U in leucogranites and Au in metasediments. This paper concerns the dating of rocks in the vicinity of the Navachab Gold Mine, 11km WSW of Karibib (Fig. 1). The Navachab deposit has been described as an example of distal skarn or sheeted-vein/skarn mineralization (Pirajno and Jacob, 1991; Pirajno *et al.*, 1991; Moore and Jacob, 1998). The mineralized rocks comprise hydrothermally altered metasediments, including schist, calc-silicate rock and marble, and quartz veins. Native gold, maldonite, scheelite and a variety of sulphides constitute the ore minerals. A variety of igneous intrusions, generally of granitic composition, are present in the vicinity of the deposit and field and geochronological work was undertaken in order to investigate whether there is any direct relationship between igneous activity and the mineralization.

Analytical Procedures

Zircon separations were carried out at the Hugh Allsopp Laboratory, University of the Witwatersrand. Handpicking was needed for samples with little, if any, zircon yield. The zircons were mounted in epoxy together with zircon standard AS3 (Duluth Complex gabbroic anorthosite; Paces and Miller, 1989) and ANU Research School of Earth Sciences standard SL13. The grains were sectioned, polished and photographed. All zircons were examined by cathodoluminescence (CL) imaging, to facilitate the selection of analytical sites

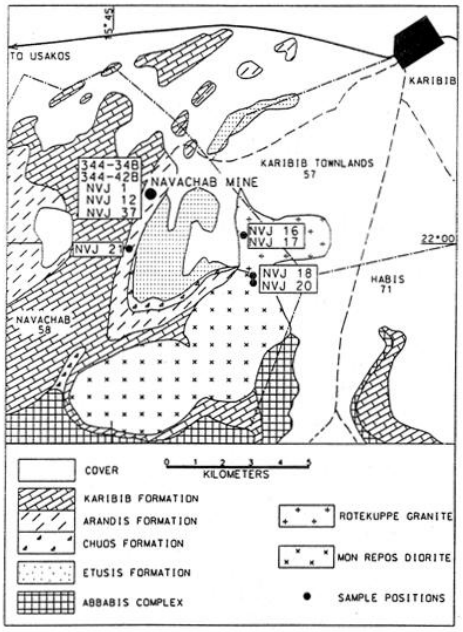

Figure 1: Simplified geological map and sample localities.

in the subsequent microprobe sessions. Through CL imaging of the zircons, hidden and complex internal structures can be more accurately determined and consequently target areas can be more reliably selected for analysis.

Reduction of SHRIMP data was conducted as described by Compston *et al.* (1992) and Williams and Claesson (1987). U/Pb in the unknowns was normalised to a $^{206*}Pb/^{238*}U$ value of 0,1859 (equivalent to an age of 1099,1 Ma) for AS3. Th and U concentrations were determined against the SL13 standard. Radiogenic $^{206*}Pb/^{238*}U$ ratios, with correction for common Pb using the measured $^{207}Pb/^{206}Pb$ and $^{206}Pb/^{238}U$ values following Tera and Wasserburg (1972), are used for young zircons such as those analysed in this study. Tera-Wasserburg concordia plots are considered more appropriate when there is no serious discordancy problem or multistage history and when reporting ages younger than 1 Ga, i.e. when measured ^{207}Pb is too imprecise for calculation of meaningful $^{207}Pb/^{206}Pb$ ages. In Tera-Wasserburg

concordia plots in this paper, the data are uncorrected for common Pb. This allows the dispersion of data to be shown relative to the common Pb content (the lower the common Pb the closer the data points plot to the concordia plot).

SHRIMP analyses on titanites were carried out on a polished thin section of sample 344-34B, and on handpicked grains from coarse crushes of NVJ12 and 344-42B. Chips of the sphene ion-microprobe standard (Khan pegmatite, Namibia) were included in the mounts and analysed sequentially with the unknowns. U/Pb ratios were normalised to a $^{206*}Pb/^{238}U$ value of 0,08367 (equivalent to an age of 518 Ma) for the Khan sphene. As for the zircons, correction for common Pb also is made using the measured $^{207}Pb/^{206}Pb$ and $^{206}Pb/^{238}U$ values following Tera and Wasserburg (1972).

Uncertainties in isotopic ratios and ages are reported at the 1σ level in the tables and in the error bars in the plotted data, but weighted mean ages calculated from pooled data sets are quoted at 95% confidence limits.

Geology and Previous Geochronology

The area investigated is located in the Central Zone of the Damara Orogen, characterised by an interference pattern of folding and granite intrusion (Smith, 1965; Miller, 1983). The rocks have been subjected to medium-grade amphibolite facies metamorphism with the common development of cordierite in metapelites, diopside and hornblende in calc-granofelses, tremolite, diopside and/or forsterite in marbles, and plagioclase, diopside and hornblende in metabasites.

The stratigraphy of the Karibib area is shown in Table 1. The oldest rocks are granitic augen ortho-gneisses and high-grade metasediments of the Palaeoproterozoic Abbabis Complex (about 2 Ga; Jacob *et al.*, 1978; Tack and Bowden, 1999). These are overlain by the Neoproterozoic Damara Supergroup which comprises Nosib and Swakop Groups. The Nosib Group (703 Ma, De Kock and Walraven, 1994) overlies the Abbabis Complex and contains a basal unit, the Etusis Formation, comprising conglomerate, meta-arkose, feldspathic quartzite and psammitic gneiss of highly variable thickness. The Etusis Formation is overlain by thin, locally developed glaciomarine meta-diamictite of the Chuos Formation (Henry, 1992). The four units of Badenhorst (1992) overlying the Chuos Formation, grouped under the heading Arandis Formation (Lehtonen *et al.*, 1996), comprise a basal interbedded calc-silicate/biotite-schist (Spes Bona Member), an interbedded marble/calc-silicate (Okawayo Member), a pelitic schist (Oberwasser Member) and some metavolcanic basic rocks (Daheim Member). A thick marble unit (Karibib Formation), follows conformably and is succeeded, through an interbedded marble/calc-silicate/pelitic schist sequence, by pelitic schists of the Kuiseb Formation. In the general Navachab area, however, the uppermost preserved formation is the Karibib marble sequence.

Table 1: Stratigraphic nomenclature of the Swakop Group and underlying basement in the Central Zone around Karibib (modified after Lehtonen *et al.*, 1996)

Formation	Member	Lithology
Kuiseb		Mainly schist
Karibib	(5 members)	Marble, calc-granofels, schist
Arandis	Daheim	Metavolcanic rocks
	Oberwasser	Schist
	Okawayo	Marble, schist, calc-granofels
	Spes Bona	Schist, calc-granofels
Chuos		Meta-diamictite, schist
Etusis		Meta-arkose, quartzite, conglomerate
Major unconformity		
Abbabis Complex		Augen gneiss, various metasediments

The Damara Supergroup in the Central Zone has been intruded by numerous syn- to post-tectonic igneous bodies of broadly granitoid composition (Kröner, 1982; Miller, 1983 and Haack *et al.*, 1983). In the general region around Karibib, the Damara granitoids include the Goas diorite suite, the Salem granite suite, a variety of red- and leuco-granites, and pegmatites and aplites. The intrusive igneous rocks within a 5km radius of the Navachab Au deposit are, in order of emplacement based on field relationships, metalamprophyre, diorite-granodiorite (Mon Repos body), red monzogranite (Rotekuppe body), pegmatite and aplite.

The rocks of the Goas diorite suite (Lehtonen *et al.*, 1995) comprise several plutons of apparently varying ages. Kröner (1982) reported Rb-Sr ages of 750 ± 35 Ma for the Palmental diorite and 651 ± 20 Ma for the younger Palmental granodiorite. De Kock and Walraven (1994) reported a zircon age of 516 ± 6 Ma for the Okongava diorite. Allsopp *et al.* (1983) reported an anomalous Rb-Sr age of 720 ± 77 Ma in the contact area of the diorite and Salem granite on Goas 79. U-Pb zircon dating of Salem granite on Goas produced an age of 580 ± 30 Ma (Allsopp *et al.*, 1983). Rb-Sr dating of Salem granites elsewhere in the Central Zone indicates apparent ages of around 550 Ma (Miller, 1983; Haack *et al.*, 1983).

A variety of red granites, commonly intrusive into the Abbabis basement or lower parts of the Damara sequence, occurs in the Central Zone. These, like the Salem granites, show a range of ages (Haack *et al.*, 1983; Miller, 1983) but little systematic dating has been done and relatively few reliable ages are available. Downing and Coward (1981) provide a Rb-Sr age of 633 ± 39 Ma and unpublished data suggest ages around 550 Ma, similar to that of the Salem granite. Red and white post-tectonic leucogranites commonly occur as cross-cutting, non-foliated intrusions in the Central Zone. They are younger than the foliated Salem and red granite types, and have Rb-Sr ages that range between 530 and 460 Ma (Haack and Gohn, 1983; Miller, 1983; Marlow, 1983). Steven *et al.* (1993) report Rb-Sr ages for leucogranites and pegmatites between 512 and 468 Ma for

the region around Omaruru and Karibib. The major leucogranitic Donkerhuk Granite batholith, which occurs along the boundary between the Central and Southern zones, has been dated by Rb-Sr techniques at 523 ± 8 Ma (Blaxland *et al.*, 1979), and Rb-Sr data on Donkerhuk pegmatites are similar (Haack and Gohn, 1988).

Many of the Rb-Sr and Pb-Pb whole rock and model ages are poorly constrained and lack the resolution necessary to decipher short-lived events or to see through metamorphism. By making use of the unique properties of the U-Pb system and the high spatial resolution of the SHRIMP this study aimed to decipher the emplacement/metamorphism and mineralization history of this small area by concentrating on dating zircon and titanite.

Sample Descriptions and Geochronological Data

Samples were collected from the Mon Repos diorite/granodiorite, the Rotekuppe monzogranite, metalamprophyre, aplite/pegmatite and quartz/skarn veins. Brief descriptions of the various samples follow.

Mon Repos diorite-granodiorite

This pluton is situated on the farm Navachab 58, about 5 km from the Navachab deposit, and is part of the Goas diorite suite (Lehtonen *et al.*, 1995). Its outcrop measures at least 10 km x 3 km. It is a zoned body and comprises diorite/quartz diorite that grades inwards to granodiorite. In places it is cut by aplite dykes. Contacts with the surrounding Karibib marbles are sharp and only minor contact metasomatic effects are recorded. The exact contact between the Mon Repos diorite and Rotekuppe granite is not clearly exposed but numerous Rotekuppe pegmatites and aplites cut the diorite near the contact, and it is evident that the diorite is older than the granite. Two samples, NVJ18 and NVJ20, were collected from the quartz diorite body, some 400 metres apart (Fig.1). Petrographically the rocks are similar. They are medium grained and exhibit igneous textures with seriate granularity and an oriented magmatic fabric in thin section. Plagioclase and hornblende are the main minerals, the former showing zoning with partly saussuritized cores, and the latter showing strongly poikilitic texture. Quartz and microcline each make up less than 10% of the rock. Small amounts of myrmekite are developed along plagioclase-microcline boundaries. Brown biotite is present as subhedral grains, generally surrounding hornblende grains. The accessory minerals include ilmenite, commonly with titanite rims, separate anhedral titanite grains, stubby apatite and zircon.

Zircons from NVJ18 are light pink in colour, clear, transparent and show euhedral facets, with no evidence of overgrowth on older cores. They form a good population for dating. Cathodoluminescence imaging reveals broad areas of uniform composition as well as compositional and sector zoning (Fig. 2). Twelve zircon grains were analysed by SHRIMP for their U-Th-Pb isotopic compositions and concentrations. The data are presented in Table 2 and plotted on a Tera-Wasserburg concordia diagram in Figure 3. With one exception (grain 8.1), all of the analyses cluster as a group near concordia, signifying low common Pb contents. The data for this group yield a weighted mean $^{206}Pb/^{238}U$ age of 546 ± 6 Ma. The single analysis which has been excluded from this calculation on statistical grounds has clearly lost Pb.

Sample NVJ 20 yielded abundant euhedral to subhedral zircons and fragments from large zircons, probably >500 μm in length. The zircons vary in colour and transparency and some have dark areas of radiation damage where high U and/or Th concentrations occur. These areas are generally very dark under cathodoluminescence, but other grains show the development of both sector and compositional zoning. Although U and Th concentrations show variation (U content: 209 to 2320 ppm), the SHRIMP U/Pb analyses show very good coherence and all 15 analyses agree within error to yield a $^{206}Pb/^{238}U$ age of 563 ± 4 Ma. The data are presented in

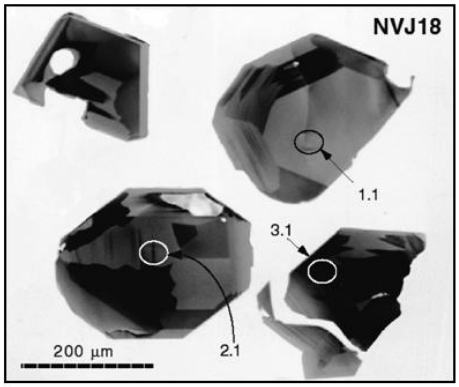

Figure 2: General population of sectioned zircons of NVJ18 as seen through SEM cathodoluminescence imaging. The zones of high U (and enhanced radiation damage) generally are seen as darker areas. Numbers and ellipses represent the locations of analyses.

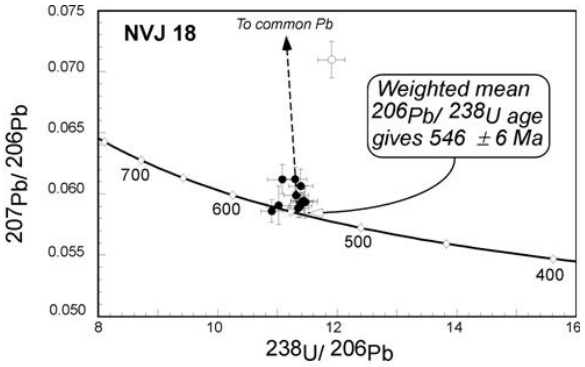

Figure 3 : Tera-Wasserburg U-Pb concordia diagram showing the SHRIMP data for the diorite sample NVJ18. The data are shown uncorrected for common Pb. The age indicated was calculated from the data shown as filled symbols. The single analysis shown as an unfilled symbol was excluded from the age calculation (see text for explanation). The concordia curve is calibrated in Ma.

Table 2: Summary of SHRIMP U-Pb zircon results for samples NVJ 18 and 20

Grain. spot	U (ppm)	Th (ppm)	Th/U	Pb* (ppm)	$^{204}Pb/^{206}Pb$	f_{206} %	Measured Ratios $^{238}U/^{206}Pb$	±	$^{207}Pb/^{206}Pb$	±	Radiogenic Ratios $^{206}Pb/^{238}U$	±	Ages (in Ma) $^{206}Pb/^{238}U$	±
NVJ 18														
1.1	218	418	1.92	27	0.000242	0.15	11.414	0.180	0.0594	0.0007	0.0875	0.0014	541	8
2.1	123	230	1.87	16	0.000383	0.11	11.018	0.199	0.0591	0.0016	0.0907	0.0016	559	10
3.1	134	188	1.41	16	0.000597	0.05	10.904	0.183	0.0586	0.0009	0.0917	0.0015	565	9
4.1	199	398	2.00	25	0.000010	0.08	11.346	0.180	0.0588	0.0008	0.0881	0.0014	544	8
5.1	140	239	1.71	17	0.000005	0.11	11.383	0.193	0.0591	0.0010	0.0878	0.0015	542	9
6.1	156	305	1.96	20	0.000188	0.30	11.392	0.204	0.0606	0.0014	0.0875	0.0016	541	9
7.1	148	300	2.03	15	0.000154	0.14	11.472	0.198	0.0593	0.0013	0.0871	0.0015	538	9
8.1	112	153	1.38	8	0.000711	1.57	11.907	0.226	0.0710	0.0015	0.0827	0.0016	512	9
9.1	122	241	1.97	12	0.000154	0.37	11.081	0.245	0.0612	0.0012	0.0899	0.0020	555	12
10.1	143	277	1.94	13	0.000270	0.16	11.444	0.221	0.0595	0.0010	0.0873	0.0017	539	10
11.1	147	262	1.78	14	0.000121	0.21	11.312	0.207	0.0599	0.0014	0.0882	0.0016	545	10
12.1	128	256	1.99	13	0.000293	0.37	11.295	0.195	0.0612	0.0010	0.0882	0.0015	545	9
NVJ 20														
1.1	774	940	1.21	89	0.000008	0.07	10.748	0.157	0.0588	0.0004	0.0930	0.0014	573	8
2.1	825	805	0.98	90	0.000059	0.12	10.768	0.160	0.0592	0.0005	0.0928	0.0014	572	8
2.2	2285	588	0.26	206	0.000001	0.04	10.868	0.154	0.0586	0.0002	0.0920	0.0013	567	8
3.1	1412	1420	1.01	153	0.000010	0.08	10.879	0.158	0.0589	0.0003	0.0919	0.0013	566	8
4.1	2320	762	0.33	210	0.000055	0.14	10.958	0.158	0.0594	0.0003	0.0911	0.0013	562	8
5.1	597	740	1.24	68	0.000097	0.21	10.926	0.184	0.0600	0.0008	0.0913	0.0015	563	9
6.1	454	506	1.11	50	0.000010	0.02	11.041	0.168	0.0585	0.0006	0.0906	0.0014	559	8
7.1	257	186	0.72	25	0.000083	0.13	11.349	0.192	0.0593	0.0008	0.0880	0.0015	544	9
8.1	341	329	0.97	36	0.000268	0.37	10.965	0.175	0.0612	0.0005	0.0909	0.0015	561	9
9.1	400	398	0.99	44	0.000007	0.14	10.790	0.162	0.0594	0.0005	0.0926	0.0014	571	8
10.1	418	541	1.29	47	0.000074	0.12	11.094	0.175	0.0593	0.0008	0.0900	0.0014	556	8
11.1	293	240	0.82	30	0.000033	0.03	11.025	0.173	0.0586	0.0007	0.0907	0.0014	560	8
12.1	738	874	1.18	85	0.000017	0.04	10.699	0.166	0.0586	0.0004	0.0934	0.0015	576	9
13.1	252	309	1.22	28	0.000074	<.01	11.325	0.204	0.0581	0.0008	0.0883	0.0016	546	9
14.1	209	147	0.70	21	0.000128	0.09	10.877	0.216	0.0590	0.0007	0.0919	0.0018	566	11

Note : Uncertainties given at the one σ level; f_{206} % denotes the percentage of ^{206}Pb that is common Pb.

Table 2 and are plotted on a Tera-Wasserburg concordia plot in Figure 4.

Rotekuppe monzogranite

This granite is situated southwest of Karibib, and <4 km ast of Navachab Mine. It is largely covered by younger sand and calcrete but forms the prominent "Rotekuppe" hill south of Karibib. The rock is medium grained and contains pegmatitic lenses and segregations and aplite dykes. The rock is a leucocratic monzogranite and exhibits a typical hypidiomorphic-granular texture with no visible directional fabric. It is younger than the Mon Repos diorite since Rotekuppe dykes cut the diorite. Typical Rotekuppe granite has a granitic/monzogranitic composition and consists of anhedral quartz, subhedral microcline with patch-perthitic texture, and subhedral zoned plagioclase displaying myrmekitic texture and albite rims. Biotite occurs in minor amounts and is slightly altered along cleavage traces to chlorite. Accessory minerals include muscovite, Fe-oxide, apatite and zircon.

The two Rotekuppe monzogranite samples (NVJ16 and NVJ17) selected for analysis were collected a few tens of metres apart from fresh outcrops 3,8 km from Navachab Mine. NVJ16 yielded abundant zircons of good quality which are lightly coloured and generally euhedral, with long prism and stubby pyramidal faces. Cathodoluminescence imaging shows well-developed compositional zoning (Fig. 5). A few rounded grains

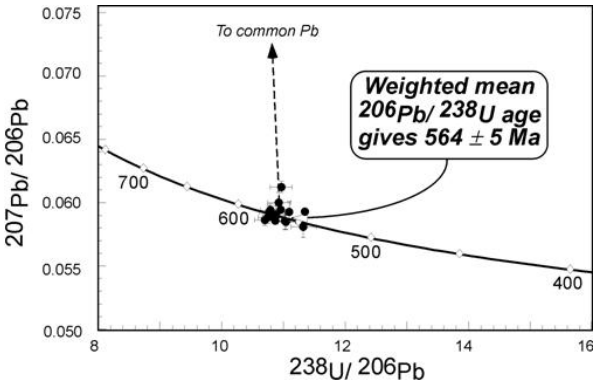

Figure 4 : Tera-Wasserburg U-Pb concordia diagram showing the SHRIMP data for sample NVJ20. The data are shown uncorrected for common Pb.

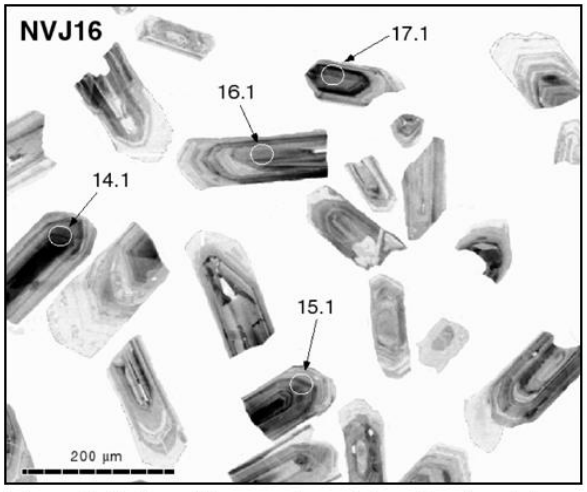

Figure 5: A view of the general population of sectioned zircons from NVJ16 as seen through SEM cathodoluminescence imaging. The zones of high U (and enhanced radiation damage) are seen as darker areas. The numbers and ellipses represent the location of analyses.

were noted, raising the possibility of some inheritance in this population. The results of 28 U-Th-Pb analyses on 27 different zircons are listed in Table 3 and the SHRIMP analyses are plotted on a Tera-Wasserburg U-Pb concordia diagram in Figure 6. The data are plotted uncorrected for common Pb. The common Pb correction points in the direction of the vector shown. The majority of the data from this sample plot on or near the concordia curve as a well-defined group showing little Pb loss and minimal common Pb. After correction for this minor common Pb component, the data combine to form a single-age population from which a weighted mean $^{206}Pb/^{238}U$ age of 543 ± 5 Ma (2σ) can be calculated. A number of analyses plot well above this group, and are off-scale on the concordia plot at the scale shown. These zircons have relatively higher common Pb contents and have also suffered significant radiogenic Pb loss. Both effects are probably related to the higher U concentrations measured within these zircons. These analyses are not included in the reported age calculation.

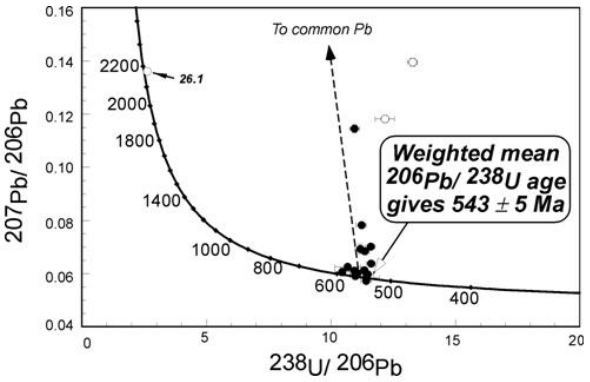

Figure 6 : Tera-Wasserburg U-Pb concordia diagram showing the SHRIMP data for the Rotekuppe monzogranite sample NVJ16. The data are shown uncorrected for common Pb. Any common Pb correction would cause the data to move down to the concordia curve along the subvertical broken line and arrow. Note that the analyses plotted as open circles were not included in the age calculation. These analyses represent either xenocrysts (26.1) or have suffered significant Pb loss.

One analysis (26.1) of a core (identified through cathodoluminescence imaging, Fig. 7) shows the presence of a substantially older component. A $^{207}Pb/^{206}Pb$ age of 2164 ± 6 Ma shows that this is an inherited core, and this age probably reflects the age of the protolith for this granite.

Zircons separated from NVJ17 are generally rather elongate, are light yellow to brown in colour, and show strong compositional zoning. Some zones have high U and Th contents and have suffered advanced radiation damage. Twenty-nine SHRIMP U-Th-U analyses were performed and the data are plotted in Figure 8 and listed in Table 4. It is apparent that the granite contains a heterogenous population of zircons showing inheritance from older basement. Some of these exotic zircons are discrete grains but they are also found as cores surrounded by zircon which crystallised during magmatism. Excluding these obviously anomalous analyses, the data set is further complicated by the dual effects of

Table 3: Summary of SHRIMP U-Pb zircon results for samples NVJ 16

							Radiogenic ratios						Ages (in Ma)						
Grain. spot	U (ppm)	Th (ppm)	Th/U	Pb* (ppm)	$^{204}Pb/^{206}Pb$	f_{206} %	$^{206}Pb/^{238}U$	±	$^{207}Pb/^{235}U$	±	$^{207}Pb/^{206}Pb$	±	$^{206}Pb/^{238}U$	±	$^{207}Pb/^{235}U$	±	$^{207}Pb/^{206}Pb$	±	% conc.
Magmatic zircons																			
1.1	433	724	1.67	52	0.00016	0.33	0.0879	0.0012					543	7					
2.1	602	375	0.62	55	0.00072	1.43	0.0850	0.0014					526	8					
3.1*	603	335	0.56	43	0.00897	15.18	0.0651	0.0084					407	51					
4.1*	1137	987	0.87	76	0.01164	20.92	0.0539	0.0029					338	18					
5.1	140	282	2.02	19	0.00001	0.26	0.0954	0.0027					587	16					
6.1*	802	479	0.60	64	0.00394	7.32	0.0762	0.0024					473	14					
7.1*	221	152	0.69	23	0.02311	35.83	0.1010	0.0128					620	75					
8.1	288	527	1.83	37	0.00060	0.32	0.0911	0.0034					562	20					
9.1*	2321	723	0.31	85	0.00969	15.55	0.0357	0.0007					226	4					
10.1	302	340	1.12	31	0.00051	0.65	0.0856	0.0013					530	8					
11.1*	889	322	0.36	66	0.01921	30.61	0.0687	0.0078					428	47					
12.1	294	314	1.07	31	0.00055	1.21	0.0869	0.0014					537	8					
13.1	361	626	1.74	45	0.00012	0.26	0.0910	0.0017					562	10					
13.2	208	334	1.61	25	0.00035	1.32	0.0883	0.0017					545	10					
14.1*	258	123	0.48	14	0.00714	13.07	0.0484	0.0008					305	5					
15.1	594	393	0.66	57	0.00021	<.01	0.0876	0.0041					541	24					
16.1	1163	375	0.32	108	0.00020	0.50	0.0932	0.0046					575	27					
17.1*	449	292	0.65	34	0.00512	9.93	0.0678	0.0010					423	6					
18.1	253	443	1.75	31	0.00002	<.01	0.0878	0.0016					543	9					
19.1	201	253	1.26	22	0.00016	0.07	0.0871	0.0017					538	10					
20.1	288	413	1.43	33	0.00104	2.34	0.0870	0.0016					538	9					
21.1	188	321	1.70	23	0.00000	0.11	0.0903	0.0019					557	11					
22.1*	988	227	0.23	46	0.00632	15.45	0.0438	0.0030					276	19					
22.2*	2491	432	0.17	112	0.00765	24.61	0.0451	0.0008					284	5					
23.1*	517	222	0.43	31	0.01463	38.36	0.0526	0.0014					331	9					
24.1	126	126	1.00	13	0.00010	0.01	0.0910	0.0018					562	10					
27.1	165	149	0.90	16	0.00327	6.78	0.0852	0.0016					527	9					
Inherited zircons																			
26.1*	490	225	0.46	203	0.00008	0.14	0.3797	0.0065	7.0682	0.1266	0.1350	0.0005	2075	30	2120	16	2164	6	96

Note: Uncertainties given at the one σ level; f_{206} % denotes the percentage of ^{206}Pb that is common Pb; % conc = % concordant, where 100% means a concordant analysis; * not included in age calculation.

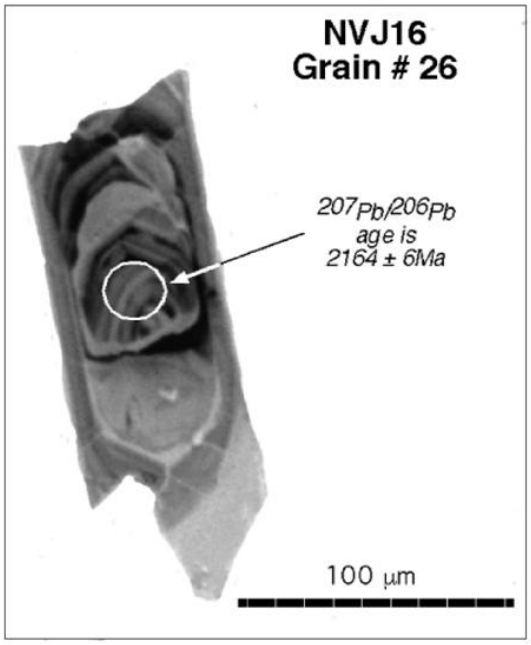

Figure 7: Cathodoluminescence image of grain 26 from sample NVJ16. SHRIMP analysis of the core shows that this is an Early Proterozoic inherited core.

radiogenic Pb loss and very high common Pb contents, probably both a consequence of deep weathering. Plagioclase in NVJ17 is more extensively saussuritised than that in NVJ16. Elimination of data indicating severe Pb loss and those with very high common Pb contents, results in a combined mean $^{206}Pb/^{238}U$ age of 539 ± 6 Ma, the interpreted crystallization age of the granite.

The inheritance pattern is also complicated by severe Pb loss, but discordant analyses of this older component yield minimum Early Proterozoic $^{207}Pb/^{206}Pb$ ages (Table 4) consistent with data obtained from other samples in this study. These exotic grains do, however, show a wide variation in geochemistry - specifically the U and Th concentrations and Th/U ratios, suggesting diverse sources.

Metalamprophyre

Metalamprophyre is exposed in the main Navachab open pit, where it occurs as semi-concordant sills along layering of marbles in the Okawayo Member. The metalamprophyre forms a single (8 m thick) sill in the southern part of the open pit but splits into 3 thinner sills in the northern part. It is a fine grained, massive, melanocratic rock displaying sharp contacts with the intruded marble, and it is cut by mineralized quartz veins containing sulphides. Near the contacts it exhibits a globular (amygdaloidal?) texture of carbonate blebs.

In thin section the metalamprophyre exhibits a metamorphic texture, similar to hornfels. It consists of small phenocrysts of hornblende (1-2 mm) and lesser poikilitic clinopyroxene in an aphanitic biotite-rich matrix. Minor plagioclase and calcite are also present in the

Table 4: Summary of SHRIMP U-Pb zircon results for sample NVJ 17

							Radiogenic ratios						Ages (in Ma)						
Grain. spot	U (ppm)	Th (ppm)	Th/U	Pb* (ppm)	$^{204}Pb/^{206}Pb$	f_{206} %	$^{206}Pb/^{238}U$	±	$^{207}Pb/^{235}U$	±	$^{207}Pb/^{206}Pb$	±	$^{206}Pb/^{238}U$	±	$^{207}Pb/^{235}U$	±	$^{207}Pb/^{206}Pb$	±	% conc.
Magmatic zircons																			
1.1	138	154	1.12	15	0.001359	0.18	0.0888	0.0021					548	12					
2.1	905	533	0.59	85	0.000330	0.51	0.0872	0.0015					539	9					
4.1	1402	651	0.46	116	0.000816	1.90	0.0814	0.0014					505	9					
5.1	1182	1261	1.07	119	0.002054	3.82	0.0837	0.0015					518	9					
6.1	511	130	0.26	43	0.001473	2.50	0.0870	0.0018					538	11					
7.1	591	493	0.83	34	0.009865	22.91	0.0443	0.0013					279	8					
8.1	333	155	0.47	31	0.000114	<.01	0.0887	0.0017					548	10					
9.1	168	244	1.46	19	0.000094	0.64	0.0851	0.0048					526	28					
10.1	272	303	1.12	23	0.005831	11.17	0.0615	0.0014					385	8					
11.1	140	328	2.34	20	0.000174	<.01	0.0916	0.0020					565	12					
12.1	91	121	1.33	10	0.000010	<.01	0.0895	0.0024					553	14					
13.1	1109	347	0.31	44	0.014380	27.31	0.0373	0.0007					236	4					
13.2	353	249	0.71	33	0.000871	1.04	0.0847	0.0016					524	10					
13.3	289	502	1.74	35	0.000918	2.05	0.0822	0.0016					509	9					
14.1	549	521	0.95	53	0.000290	0.65	0.0816	0.0016					506	9					
15.1	351	416	1.19	38	0.001151	1.57	0.0875	0.0017					540	10					
17.1	416	163	0.39	34	0.001592	2.40	0.0801	0.0015					497	9					
18.1	620	515	0.83	56	0.001330	2.13	0.0772	0.0015					479	9					
20.1	661	180	0.27	54	0.004266	7.81	0.0814	0.0015					505	9					
21.1	709	270	0.38	39	0.001060	1.54	0.0541	0.0010					340	6					
22.1	145	404	2.78	15	0.002834	6.10	0.0742	0.0017					461	10					
23.1	4060	1147	0.28	334	0.006480	11.96	0.0828	0.0014					513	8					
24.2	440	150	0.34	39	0.000176	0.28	0.0881	0.0017					545	10					
Inherited zircons																			
3.1	433	109	0.25	108	0.000239	0.43	0.2513	0.0047	3.926	0.083	0.1133	0.0009	1445	24	1619	17	1853	14	78
3.2	4841	1775	0.37	254	0.013649	24.35	0.0445	0.0015	0.686	0.143	0.1120	0.0226	280	9	531	90	1832	420	15
15.2	344	238	0.69	28	0.006494	11.59	0.0630	0.0014	0.838	0.084	0.0965	0.0092	394	8	618	47	1557	189	25
16.1	789	139	0.18	137	0.004309	7.69	0.1738	0.0031	2.965	0.182	0.1237	0.0070	1033	17	1399	48	2011	104	51
19.1	2099	659	0.31	143	0.019393	34.60	0.0501	0.0015	1.157	0.061	0.1675	0.0068	315	9	780	29	2533	70	12
24.1	1061	17	0.02	283	0.000077	0.14	0.2792	0.0094	4.192	0.313	0.1089	0.0068	1587	47	1672	63	1781	119	89

Note : . Uncertainties given at the one σ level; f_{206} % denotes the percentage of ^{206}Pb that is common Pb; % conc = % concordant, where 100% means a concordant analysis; * not included in age calculation.

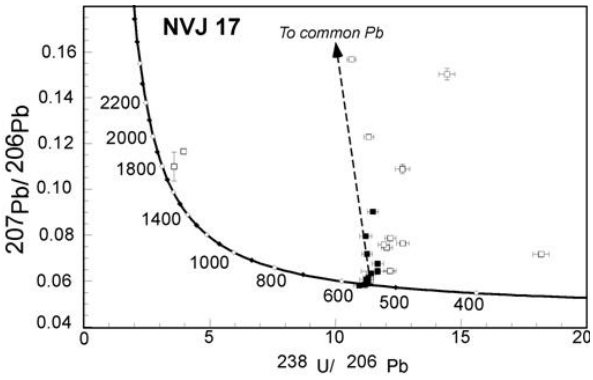

Figure 8: Tera-Wasserburg U-Pb concordia diagram showing the SHRIMP data for the granite sample NVJ17. The data are shown uncorrected for common Pb. The age indicated was calculated from the data shown as filled symbols (see text for explanation).

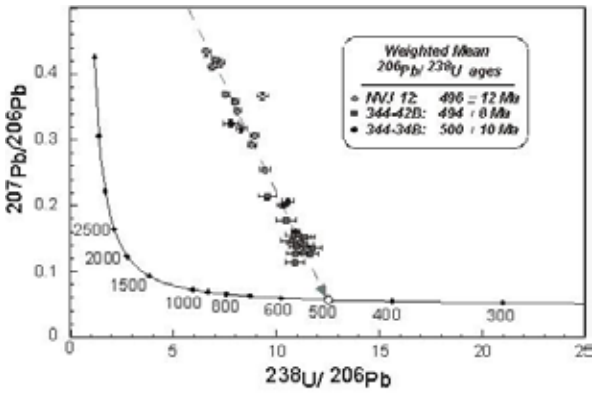

Figure 9: Tera-Wasserburg U-Pb concordia diagram showing the SHRIMP data for the metalamprophyre sample NVJ12 and the quartz/skarn veins 344-42B and 344-34B, plotted uncorrected for common Pb. The data are plotted with 95% confidence level error bars.

matrix, together with accessory apatite, titanite and ilmenite, the latter generally with rims of titanite. No zircon was observed. Sample NVJ12 yielded small clear, anhedral titanite grains. Five U-Pb SHRIMP analyses were performed on four titanite grains. The data are plotted in Figure 9 and listed in Table 5. The computed weighted mean $^{206}Pb/^{238}U$ age is 496 ± 12 Ma (MSWD = 1.05).

Aplite/Pegmatite

Aplite and pegmatite are observed in the Navachab open pit as thin, vertical dykes trending WNW. They generally lie parallel to the J3 joint set of the Navachab pit, locally are slightly boudinaged, and in places they either occupy fault planes or are offset by small faults. They represent the only granitic rocks that intersect the

Table 5: Summary of SHRIMP U-Pb titanite results for samples, NVJ 12, 344-34B and 344-42B

Grain. spot	U (ppm)	Th (ppm)	Th/U	Pb* (ppm)	$^{204}Pb/^{206}Pb$	f_{206} %	Radiogenic Ratios $^{206}Pb/^{238}U$	±	Ages (in Ma) $^{206}Pb/^{238}U$	±
Sample 344-34B										
1.1	31	13	0.42	3	0.00341	8.65	0.0835	0.0030	517	18
2.1	20	13	0.64	2	0.00909	14.79	0.0811	0.0037	502	22
3.1	34	9	0.27	3	0.00534	8.77	0.0804	0.0026	499	16
4.1	25	8	0.30	2	0.00927	11.73	0.0780	0.0029	484	18
5.1	40	11	0.26	3	0.00504	9.59	0.0768	0.0030	477	18
6.1	40	17	0.44	3	0.00594	11.96	0.0811	0.0029	503	17
7.1	26	7	0.26	2	0.00700	11.59	0.0776	0.0034	482	21
8.1	32	12	0.39	3	0.00696	9.84	0.0819	0.0028	508	17
9.1	33	13	0.40	3	0.00616	10.51	0.0818	0.0030	507	18
10.1	53	12	0.23	4	0.00359	6.96	0.0851	0.0035	527	21
11.1	16	11	0.73	1	0.01043	19.28	0.0841	0.0040	520	24
12.1	26	12	0.47	2	0.00536	10.93	0.0828	0.0038	513	23
13.1	36	9	0.26	3	0.00491	8.45	0.0785	0.0025	487	15
14.1	21	10	0.46	2	0.00603	10.18	0.0789	0.0030	489	18
Sample NVJ 12										
2.1	24	6	0.24	2	0.01624	30.7	0.0774	0.0018	480	11
3.1	14	6	0.43	1	0.02336	38.0	0.0663	0.0021	414	12
4.1	12	7	0.60	1	0.02292	44.3	0.0765	0.0025	475	15
5.1	17	10	0.57	1	0.02725	44.9	0.0783	0.0021	486	13
6.1	32	17	0.53	3	0.01273	24.3	0.0801	0.0022	497	13
7.1	16	5	0.31	1	0.01939	37.0	0.0787	0.0019	489	12
8.1	23	17	0.70	2	0.01497	29.0	0.0806	0.0018	500	11
9.1	11	5	0.43	1	0.02444	46.3	0.0815	0.0027	505	16
10.1	21	20	0.93	2	0.01918	35.3	0.0797	0.0018	495	11
11.1	12	6	0.49	1	0.02069	43.4	0.0819	0.0025	508	15
12.1	19	8	0.43	1	0.02082	38.3	0.0817	0.0020	506	12
Sample 344-42B										
1.1	15	6	0.37	1	0.00628	17.6	0.0799	0.0021	496	12
2.1	11	4	0.38	1	0.01997	32.9	0.0862	0.0043	533	26
1.2	13	5	0.38	1	0.00652	18.3	0.0773	0.0022	480	13
3.1	30	5	0.15	2	0.00291	12.7	0.0799	0.0016	495	10
4.1	9	2	0.18	1	0.01665	32.0	0.0820	0.0027	508	16

Note : 1. Uncertainties given at the one σ level; 2. f_{206} % denotes the percentage of ^{206}Pb that is common Pb.

mineralization. The dykes are mainly aplitic in character with pegmatitic segregations in places. They are younger than, and cut across the lamprophyre. Most aplites cut the mineralised quartz veins, and therefore post-date the mineralization, whereas a few are cut by quartz veins, and are therefore older.

Sample NVJ1 is an aplite from the open pit, and NVJ37 is a finer grained part of a pegmatite from a borehole (N240) drilled just north of the open pit. The main minerals are quartz, perthitic microcline and albite, commonly in the form of oriented laths. Also present are muscovite, apatite, topaz, blue tourmaline and calcite in late veinlets. In places graphite is present. These rocks provided very poor material for dating and contain extremely rare zircons of very poor quality. A few zircons from sample NVJ1 show variable morphology from totally opaque and metamict to some small slightly rounded grains and fragments.

U-Pb SHRIMP analyses of 7 zircons from NVJ1 show an extreme range in U concentrations (170 to 39000 ppm) and considerable variation in Th/U. No conclusive geochronological constraints can be placed on the emplacement age. There is clearly an older Palaeoproterozoic inherited zircon component (Table 6) and also Pb loss. Perhaps the best estimate is the $^{207}Pb/^{206}Pb$ age of 564 ± 30 Ma (2σ) for one of the analyses (3.1). This age, however, is considered unreliable as the Pb/U calibration for a zircon with almost 4% U is not robust. Apart from the fact that this particular zircon must also be inherited, there is a systematic bias in ion microprobe analyses towards higher apparent Pb/U ages in zircons with such extreme compositions (Williams and Hergt, 2000) and it is probable that this analysis is highly discordant. Furthermore, the indicated age would make this aplite the oldest of all the igneous rocks sampled, when the cross-cutting field relationships demonstrate that it is actually the youngest.

Sample NVJ37 yielded a few squat, euhedral zircons which are grey to milky, and opaque, indicating high radioactive-element concentrations and metamictization. Only four analyses were obtained from this population (Table 6). Analysis showed very high to extreme U concentrations, although Th concentrations and Th/U ratios are low. Regression of the data (corrected for common Pb using measured ^{208}Pb) gives an upper intercept age of 544 ± 39 Ma (MSWD = 0,42) and a lower intercept of 36 ± 44 Ma. This age is again anomalous in terms of the observed field relationships, and considering the paucity of zircons and data, the question of inheritance, and the extreme alteration of the few zircons present, no great significance must be attached to this age.

Mineralized quartz veins

The Navachab ore deposit, a sheeted quartz vein-distal skarn type deposit, is described elsewhere (Pirajno and Jacob, 1991; Moore and Jacob, 1998) and only the geochronological aspects are considered here. The veins consist largely of quartz. Besides sulphides (pyrite, pyrrhotite) and gold, they also contain minor carbonate, clinopyroxene, biotite and sphene. They are younger than the metalamprophyre sill and cut through it but, generally, are older than the aplite/pegmatite dyke set.

Two vein samples containing euhedral titanite were selected for analysis from borehole N344 (samples 344-42B and 344-34B). Eleven different titanites were analysed from sample 344-42B. The data are shown in Table 5 and all but one of the analyses combine to give a weighted mean $^{206}Pb/^{238}U$ age of 494 ± 8 Ma (MSWD = 0.72). The data for this sample and for NVJ12 are plotted in Figure 9 as measured ratios, and fall along a well-constrained mixing line between the radiogenic end-member composition (on the concordia) and a common Pb composition. All analyses show significant common Pb contents.

In sample 344-34B, coarse-grained titanite containing numerous inclusions has grown in the margins of the vein. Fourteen points were analysed. The U-Pb SHRIMP analyses (Table 5) are plotted on a Tera-Wasserburg U-Pb concordia diagram in Figure 9. A weighted mean $^{206}Pb/^{238}U$ age of 500 ± 10 Ma (MSWD = 0.63) is calculated for all 14 data points.

Table 6: Summary of SHRIMP U-Pb zircon results for samples NVJ 1 and NVJ 37

							Radiogenic ratios						Ages (in Ma)						
Grain spot	U (ppm)	Th (ppm)	Th/U	Pb* (ppm)	$^{204}Pb/^{206}Pb$	f_{206} %	$^{206}Pb/^{238}U$	±	$^{207}Pb/^{235}U$	±	$^{207}Pb/^{206}Pb$	±	$^{206}Pb/^{238}U$	±	$^{207}Pb/^{235}U$	±	$^{207}Pb/^{206}Pb$	±	% conc.
NVJ 1																			
1.1	212	171	0.81	95	0.000003	0.006	0.3840	0.0065	6.725	0.1225	0.1270	0.0006	2095	30	2076	16	2057	9	102
2.1	6681	42	0.01	187	0.000049	0.087	0.0309	0.0006	0.224	0.0047	0.0527	0.0004	196	4	205	4	314	19	63
3.1	38945	510	0.01	3010	0.000012	0.022	0.0846	0.0019	0.687	0.0164	0.0589	0.0004	523	11	531	10	564	15	93
4.1	170	100	0.59	60	0.000691	1.233	0.3111	0.0073	5.624	0.1775	0.1311	0.0024	1746	36	1920	28	2113	33	83
5.1	192	111	0.57	81	0.001146	2.044	0.3647	0.0065	6.850	0.2036	0.1362	0.0029	2005	31	2092	27	2180	38	92
6.1	200	151	0.75	83	0.000033	0.060	0.3611	0.0069	6.147	0.1266	0.1235	0.0007	1987	33	1997	18	2007	10	99
7.1	4868	12	0.00	109	0.000122	0.217	0.0247	0.0006	0.187	0.0052	0.0550	0.0006	157	4	174	4	412	22	38
NVJ 37																			
1.1	1811	10	0.01	133	0.000207	0.348	0.0002	0.0804	0.0034	0.648	0.028	0.0585	498	20	507	18	547	18	26
2.1	4471	159	0.04	141	0.001234	2.053	0.0005	0.0345	0.0005	0.272	0.005	0.0572	218	3	244	4	500	22	27
3.1	10456	51	0.00	584	0.000160	0.326	0.0012	0.0614	0.0026	0.490	0.051	0.0579	384	16	405	35	525	##	27
4.1	3462	28	0.01	183	0.002242	4.173	0.0006	0.0580	0.0009	0.456	0.011	0.0571	363	5	382	8	496	39	28

Note : . Uncertainties given at the one σ level; f_{206} % denotes the percentage of ^{206}Pb that is common Pb; % conc = % concordant, where 00% means a concordant analysis; * not included in age calculation; data for sample NVJ 37 are corrected for common Pb using the ^{208}Pb correction.

Calc-silicate country rock

One sample (NVJ21) of calc-silicate country rock was collected from the Spes Bona Member well away from the site of mineralization, 2 km to the south of the open pit. The rock is aphanitic and banded, with hornblende poikiloblasts in a matrix comprising plagioclase and biotite. Accessory quartz, titanite, opaque minerals and zircon are present. Only a few zircons were extracted from this rock and from their rounded and pitted appearance, they are detrital in origin. Only four analyses were obtained on three suitable zircon grains from this rock (Table 7). All the data are discordant and two of the analyses yield minimum $^{207}Pb/^{206}Pb$ ages of approximately 2400 Ma. Of interest are two analyses on a grain whose cathodoluminescence image shows an older core and younger overgrowth. The core yields a late Archaean $^{207}Pb/^{206}Pb$ age of 2872 ± 4 Ma and the overgrowth an Early Proterozoic age of 1962 ± 10 Ma. The youngest detrital zircon (1962 ± 10 Ma) gives an approximation of the minimum age for the source rock of the zircon. The Archaean age is of interest because recently Seth *et al.* (1998) have reported Archaean ages from pre-Damara basement granitic gneisses in the Kaoko belt, NW Namibia, in the range 2645 to 2585 Ma.

Discussion and Conclusions

Episodes of granitoid intrusion, metamorphism and tectonic activity took place over an extended period from about 650 Ma to 460 Ma in the Damaran Orogen. Early syntectonic granitoids associated with D_1/D_2 deformational events, record ages between 650 Ma and 590 Ma (Miller, 1983), largely from the northern margin of the orogen. The major period of intrusion of syn- to late-tectonic granites in the Central Zone was around 550 Ma (Miller, 1983; Steven *et al.*, 1993). Regional metamorphism accompanied and outlasted both deformation and granite intrusion. There is disagreement on the precise timing of the peak of regional metamorphism in the Central Zone, with estimates ranging from 540 Ma to 520 Ma (Kröner, 1982; Haack and Martin, 1983; Steven 1993).

Tectonic activity and granite intrusion continued in the Southern Zone, terminating there at around 525 Ma with the intrusion of the Donkerhuk Granite (Miller, 1983). However, high-temperature conditions, particularly in the Central Zone, apparently persisted until about 460 Ma, associated with the emplacement of late leucogranite, alaskite (Rössing Mine) and pegmatite (Miller, 1983; Steven *et al.*, 1993). Steven (1993) has pointed out that metamorphism in the Central Zone, comprising both regional and contact metamorphism, was diachronous, that it is difficult to set an exact date for the peak of regional metamorphism, and that the heat supplied by the regional metamorphism and intrusive granites resulted in the prolonged period over which temperatures remained elevated.

In the Navachab area, the present study has revealed two distinct age clusters around 550 Ma and 500 Ma. The former represents the age of granitoid intrusion, and the latter some subsequent metamorphic age. The Mon Repos diorite, emplaced around 550 Ma, and the Rotekuppe granite, at about 540 Ma, are identified as typical examples of D3-related syntectonic granitoids of the Central Zone.

Titanite grains in the metalamprophyric sill in the Navachab pit have formed as metamorphic overgrowths on ilmenite grains. Titanite is known to be reactive during metamorphism and the U/Pb ages of 496 Ma may record new growth during metamorphism or a fluid-related reaction associated with the mineralization. This age is indistinguishable from those for titanite in mineralized quartz/skarn veins in the Navachab deposit, at 494 Ma to 500 Ma (Fig. 9). The timing of mineralization may be interpreted from this evidence in two ways. Either 500 Ma represents the age of mineralization during which hydrothermal titanite crystallised, or the mineralization occurred at an earlier date, and the age represents metamorphic recrystallisation of titanite. The latter option appears to be the most logical, particularly given the deformed nature of the quartz veins (boudinaged, folded, rotated garnets in wallrock skarn).

Pegmatite and aplite veins in the Spes Bona Member in the Navachab pit and in the Etusis Formation on the ridge to the east, are observed to cut the mineralized vein system. Poorly constrained apparent ages of between 544 Ma and 564 Ma obtained for these rocks on highly altered zircons have large uncertainties between 30 – 40 Ma. Given these large errors, possible analytical problems with the Pb/U calibration and even the possibility that these zircons could be xenocrystic, it is difficult to deduce from these data whether the pegmatites are related to the intrusion of the granitic rocks, or to

Table 7: Summary of SHRIMP U-Pb zircon results for samples NVJ 21

							Radiogenic ratios						Ages (in Ma)						
Grain. spot	U (ppm)	Th (ppm)	Th/U	Pb* (ppm)	$^{204}Pb/^{206}Pb$	f_{206} %	$^{206}Pb/^{238}U$	±	$^{207}Pb/^{235}U$	±	$^{207}Pb/^{206}Pb$	±	$^{206}Pb/^{238}U$	±	$^{207}Pb/^{235}U$	±	$^{207}Pb/^{206}Pb$	±	% conc.
NVJ 21																			
1.1	917	536	0.58	242	0,000116	0.21	0.2271	0.0037	4.737	0.080	0.1513	0.0005	1319	19	1774	14	2360	5	56
2.1	482	302	0.63	294	0,000001	<0.01	0.5078	0.0085	14.405	0.248	0.2057	0.0005	2647	37	2777	17	2872	4	92
2.1	481	300	0.62	288	0,000001	<0.01	0.4996	0.0084	14.154	0.249	0.2055	0.0007	2612	36	2760	17	2870	6	91
2.2	237	172	0.73	94	0,000042	0.08	0.3455	0.0063	5.733	0.113	0.1204	0.0007	1913	30	1936	17	1962	10	98
3.1	562	340	0.60	171	0,000034	0.06	0.2579	0.0044	5.598	0.104	0.1574	0.0008	1479	23	1916	16	2428	9	61

Note : . Uncertainties given at the one σ level; f_{206} % denotes the percentage of ^{206}Pb that is common Pb; % conc = % concordant, where 100% means a concordant analysis.

subsequent partial melting at a later metamorphic peak. It is conceivable that the zircon ages constrain the age of granite intrusion, mineralization and pegmatite/aplite formation to around 550 Ma, and that the titanite ages represent metamorphism of the area through the new growth of titanite some 50 Ma later at 500 Ma.

An alternative interpretation is that growth of titanite occurred essentially during prograde regional metamorphism. Under these conditions, peak regional metamorphism would have occurred at 500 Ma, significantly post-dating the major granite intrusion (and heat-generating) event. Mineralization at Navachab would be directly related to the metamorphic episode, and also much younger than the intrusive granitoids. It would also require total rejection of the pegmatite/aplite age data. A very late, post-tectonic age for the regional metamorphic peak would appear to contradict the observation that geothermal gradients (e.g. andalusite-sillimanite) are readily observed around intrusive granites (Steven, 1993).

Given that many relatively young ages (515 Ma to 458 Ma) for pegmatite and alaskite mineralization in the Central Zone of the Damaran Orogen were obtained by whole-rock and mineral Rb-Sr methods (see summary in Steven *et al.*, 1993, and Tack and Bowden, 1999), the ages should be interpreted with caution as they too may represent later tectono-metamorphic events (see Clark, 1982). These young ages imply that the pegmatites and alaskites significantly postdate the main structural and intrusive events in the Central Zone by up to 90 Ma, whereas field observations frequently indicate otherwise. The truth, in this instance, would appear to lie in the field - a paradigm that was close to the heart of Henno Martin.

Acknowledgements

We thank Anglo-American Corporation for financial support for this study, and Roy Corrans in particular for his help. We thank Johan Kruger for the use of mineral separation facilities at the Hugh Allsopp Laboratory, University of the Witwatersrand, the RSES Isotope Laboratory support staff at ANU for their help, and Laurent Ameglio and Eric Ferré who helped to resolve computer problems. A special thank you is due to Frik and Juanita Badenhorst for their hospitality and support during fieldwork.

References

Allsopp, H.L., Barton, E.S., Kröner, A., Welke, H.J. and Burger, A.J. 1983. Emplacement versus inherited isotopic age patterns: a Rb-Sr and U-Pb study of Salem-type granites in the central Damara belt, 281-287. *In*: Miller, R.McG. (ed.) *Evolution of the Damara Orogen of South-West Africa/Namibia*. Spec. Publ., Geol. Soc. S. Afr., **11**, 515 pp.

Badenhorst, F.P. 1992. *The Lithostratigraphy of area 2115B and D in the Central Zone of the Damara Orogen, Namibia: with emphasis on facies changes and correlation*. Unpubl. MSc thesis, Univ. Port Elizabeth, 124 pp.

Blaxland, A., Gohn, E., Haack, U. and Hoffer, E. 1979. Rb/Sr ages of late-tectonic granites in the Damara Orogen, South-West Africa/Namibia. *N. Jb. Miner. Mh.*, **1979**, 498-508.

Clark, G.S. 1982. Rubidium-strontium isotope systematics of complex granite pegmatites, 347-371. *In*: Cerny, P. (ed.) *Granitic Pegmatites in Science and Industry.* Mineralog. Assoc. Can. Short Course Handb., **8**, 555 pp.

Compston, W., Williams, I.S., Kirschvink, J.L., Zhang, Z. and Ma, G. 1992. Zircon U-Pb ages for the Early Precambrian time-scale. *J. geol. Soc., London*, **149**, 171-184.

Deer, W.A., Howie, R.A. and Zussman, J. 1982. *Rock-forming Minerals*. Vol.1A: Orthosilicates. Longman, London, 919 pp.

de Kock, G.S. and Walraven, F. 1994. The age and geochemistry of some syn-depositional and early tectonic magmatic rocks southeast of Karibib. *Abstr. Int. Conf. on Proterozoic crustal and metallogenic evolution, Geol. Soc. and Geol. Surv. Namibia*, **13**.

Downing, K. and Coward, M.P. 1981. The Okahandja Lineament and its significance for Damaran tectonics in Namibia. *Geol. Rdsch.*, **70**, 972-1000.

Haack, U. and Gohn, E. 1988. Rb-Sr data on some pegmatites in the Damara Orogen (Namibia). *Communs geol. Surv. S.W.Afr./Namibia*, **4**, 13-17.

Haack, U. and Martin, H. 1983. Geochronology of the Damara Orogen - a review, 839-845. *In*: Martin, H. and Eder, F.W. (eds) *Intracontinental Fold Belts*. Springer Verlag, Berlin, 945 pp.

Haack, U., Hoefs, J. and Gohn, E. 1983. Genesis of Damaran granites in the light of Rb/Sr and $\delta^{18}O$ data, 847-872. *In*: Martin, H. and Eder, F.W. (eds) *Intracontinental Fold Belts*. Springer Verlag, Berlin, 945 pp.

Henry, G. 1992. *The sedimentary evolution of the Damara Sequence in the lower Khan River Valley, Namibia*. Unpubl. Ph.D. thesis, Univ. Witwatersrand, 217 pp.

Jacob, R.E., Kröner, A. and Burger, A.J. 1978. Areal extent and first U-Pb age of the pre-Damara Abbabis complex in the central Damara belt of South-West Africa. *Geol. Rdsch.*, **67**, 157-172.

Kröner, A. 1982. Rb-Sr geochronology and tectonic evolution of the Pan-African Damara belt of Namibia, South-western Africa. *Am. J. Sci.*, **282**, 1471-1507.

Lehtonen, M.I., Manninen, T.E.T. and Schreiber, U.M. 1995. Geological map of Namibia, sheet 2214 - Walvis Bay. *Geol. Surv. Namibia*, Windhoek.

Lehtonen, M.I., Manninen, T.E.T. and Schreiber, U.M. 1996. Report: lithostratigraphy of the area between the Swakop, Khan and lower Omaruru rivers, Namib Desert. *Communs geol. Surv. Namibia*, **11**, 65-75.

Marlow, A.G. 1983. Geology and Rb-Sr geochronology of mineralized and radioactive granites and alaskites, Namibia, 289-298. *In*: Miller, R.McG. (ed.) *Evolution of the Damara Orogen of South-West Africa/ Namibia*. Spec. Publ. geol. Soc. S. Afr., **11**, 515 pp.

Martin, H. 1965. *The Precambrian geology of South West Africa and Namaqualand*. Precambr. Res. Unit, Univ. Cape Town. Rustica Press, Wynberg, 159 pp.

Miller, R.McG. 1983. The Pan-African Damara Orogen of South West Africa/Namibia, 431-515. *In*: Miller, R.McG. (ed.) *Evolution of the Damara Orogen of South-West Africa/Namibia*. Spec. Publ. geol. Soc. S. Afr., **11**, 515 pp.

Moore, J.M. and Jacob, R.E. 1998. The Navachab sheeted-vein/skarn Au deposit, Namibia. *Abstr. Conf. geol. Assoc. Canada/Mineral. Assoc. Canada*, A125-A126.

Paces, J.B. and Miller, J.D. 1989. Precise U-Pb ages of Duluth Complex and related mafic intrusions, northeastern Minnesota: geochronological insights to physical, petrogenic, palaeomagnetic and tectonomagmatic processes associated with the 1,1 Ga midcontinent rift system. *J. geophys. Res*., **98B**, 13997-14013.

Pirajno, F. and Jacob, R.E. 1991. Gold mineralization in the intracontinental branch of the Damara Orogen, Namibia: a preliminary survey. *J. Afr. Earth Sci*., **13**, 305-311.

Pirajno, F., Jacob, R.E. and Petzel, V.F.W. 1991. Distal skarn-type mineralization in the Central Zone of the Damara Orogen, Namibia, 95-100. *In*: Ladeira, E.A. (ed.) *Proceedings of Brazil Gold '91: an International Symposium on the Geology of Gold: Belo Horizonte*. Balkema, Rotterdam, 823p.

Seth, B., Kröner, A., Mezger, K., Nemchin, A.A., Pidgeon, R.T. and Okrusch, M. 1998. Archaean to Neoproterozoic magmatic events in the Kaoko belt of NW Namibia and their geodynamic significance. *Precambr. Res.*, **92**, 341-363.

Smith, D.A.M. 1965. The geology of the area around the Khan and Swakop Rivers in S.W.A. *Mem. geol. Surv. S. Afr., S.W. Afr. Series*, **3**, 113 pp.

Steven, N.M. 1993. A study of epigenetic mineralization in the central zone of the Damara Orogen, Namibia, with special reference to gold, tungsten, tin and rare-earth elements. *Mem. geol. Surv. Namibia*, **16**, 166 pp.

Steven, N.M., Armstrong, R.A. and Moore, J.M. 1993. New Rb-Sr data from the Central Zone of the Damara Orogen, Namibia. *Communs geol. Surv. Namibia*, **8**, 5-14.

Tack, L. and Bowden, P. 1999. Post-collisional granite magmatism in the central Damaran (Pan-African) Orogenic Belt, western Namibia. *J. Afr. Earth Sci.*, **28**, 653-674.

Tera, F. and Wasserburg, G.J. 1972. U-Th-Pb systematics in three Apollo 14 basalts and the problem of initial Pb in lunar rocks. *Earth Planet. Sci. Lett.*, **14**, 281-304.

Williams, I.S. and Claesson, S. 1987. Isotopic evidence for the Precambrian provenance and Caledonian metamorphism of high-grade paragneisses from the Seve Nappes, Scandinavian Caledonides. II. Ion microprobe zircon U-Th-Pb. *Contrib. Mineral. and Petrol.*, **97**, 205-217.

Williams, I.S. and Hergt, J.M. 2000. U-Pb dating of Tasmanian dolerites: a cautionary tale of SHRIMP analyses of high-U zircon. *In*: Woodhead, J.D., Hergt, J.M. and Noble, W.P. (Eds.). *Beyond 2000: New frontiers in Isotope Geoscience, Lorne, 2000; Abstr. and Proc*.